University of Nebraska - Lincoln
DigitalCommons@University of Nebraska - Lincoln

Publications, Agencies and Staff of the U.S. Department of Commerce

U.S. Department of Commerce

2004

Stratospheric Aerosol Sampling: Effect of a Blunt-Body Housing on Inlet Sampling Characteristics

S. Dhaniyala
Clarkson University, Potsdam, New York, sdhaniya@clarkson.edu

P. O. Wennberg
California Institute of Technology, Pasadena, California

R. C. Flagan
California Institute of Technology, Pasadena, California

D. W. Fahey
University of Colorado, Boulder

M. J. Northway
NOAA Aeronomy Laboratory, Boulder, Colorado,

See next page for additional authors

Follow this and additional works at: http://digitalcommons.unl.edu/usdeptcommercepub

Dhaniyala, S.; Wennberg, P. O.; Flagan, R. C.; Fahey, D. W.; Northway, M. J.; Gao, R. S.; and Bui, T. P., "Stratospheric Aerosol Sampling: Effect of a Blunt-Body Housing on Inlet Sampling Characteristics" (2004). *Publications, Agencies and Staff of the U.S. Department of Commerce*. 523.
http://digitalcommons.unl.edu/usdeptcommercepub/523

This Article is brought to you for free and open access by the U.S. Department of Commerce at DigitalCommons@University of Nebraska - Lincoln. It has been accepted for inclusion in Publications, Agencies and Staff of the U.S. Department of Commerce by an authorized administrator of DigitalCommons@University of Nebraska - Lincoln.

Authors
S. Dhaniyala, P. O. Wennberg, R. C. Flagan, D. W. Fahey, M. J. Northway, R. S. Gao, and T. P. Bui

This article is available at DigitalCommons@University of Nebraska - Lincoln: http://digitalcommons.unl.edu/usdeptcommercepub/523

Aerosol Science and Technology, 38:1080–1090, 2004
Copyright © American Association for Aerosol Research
ISSN: 0278-6826 print / 1521-7388 online
DOI: 10.1080/027868290885818

This article is a US government work and is not subject to copyright in the United States.

Stratospheric Aerosol Sampling: Effect of a Blunt-Body Housing on Inlet Sampling Characteristics

S. Dhaniyala,[1] P. O. Wennberg,[2] R. C. Flagan,[3] D. W. Fahey,[4] M. J. Northway,[5,*] R. S. Gao,[5] and T. P. Bui[6]

[1]*Department of Mechanical and Aeronautical Engineering, Clarkson University, Potsdam, New York, USA*
[2]*Divisions of Geological and Planetary Sciences and Engineering and Applied Science, California Institute of Technology, Pasadena, California, USA*
[3]*Division of Chemical and Chemical Engineering, California Institute of Technology, Pasadena, California, USA*
[4]*NOAA Aeronomy Laboratory, Boulder, CO and Cooperative Institute for Research in Environmental Sciences, University of Colorado, Boulder, Colorado, USA*
[5]*NOAA Aeronomy Laboratory, Boulder, Colorado, USA*
[6]*NASA Ames Research Center, Moffett Field, California, USA*

During a campaign to study ozone loss mechanisms in the Arctic stratosphere (SOLVE), several instruments on NASA's ER-2 aircraft observed a very low number density (0.1 l^{-1}) of large, nitric-acid-containing particles that form the polar stratospheric clouds (PSCs). For effective physical and chemical characterization of these particles, the measurements from these instruments have to be intercompared and integrated. In particular, proper interpretation requires knowledge of the sampling characteristics of the particles into the instruments. Here, we present the calculation of the sampling characteristics of the one of the instruments on the ER-2, the NOAA NOy instrument. This instrument sampled ambient particles and gas from two forward-facing inlets located fore and aft on a particle-separation housing (the football) and measured total NOy in the sample. In recent studies, ambient aerosol mass has been estimated by the difference of the measurements of the two inlets with the assumption that the rear inlet observations represent the gas-phase NOy and small particles and the front inlet samples represent gas-phase NOy and all particle sizes with varied efficiency (anisokinetic sampling). This knowledge was derived largely from semiempirical relations and potential flow studies of the housing. In our study, we used CFD simulations to model the compressible flow conditions and considered noncontinuum effects in calculating particle trajectories. Our simulations show that the blunt body housing the inlets has a strong and complex interaction with the flow and particles sampled by the two inlets. The simulations show that the front inlet characteristics are influenced by the effect of the blunt body on the upstream pressure field. The rear inlet sampling characteristics are influenced both by the shape and size of the inlet and its location on the blunt body. These interactions result in calculated inlet characteristics that are significantly different from previously assumed values. Analysis of the SOLVE data, considering the ambient conditions and the calculated inlet sampling characteristics, in conjunction with thermodynamic growth modeling of super-cooled ternary solution (STS) particles, provides validation of the CFD results.

Received 18 February 2004; accepted 2 September 2004.
The authors would like to thank NASA Dryden for providing the photographs of the ER-2 and the NO_y instrument shown in Figure 1.We would like to thank the SOLVE team for the technical and logistical help during the campaign. P. O. Wennberg thanks NASA's UARP for funding support.
*Currently at Aerodyne Corp.
Address correspondence to Suresh Dhaniyala, Department of Mechanical and Aeronautical Engineering, Clarkson University, MAE Dept., Box 5725, Clarkson University, Potsdam, NY 13699, USA. E-mail: sdhaniya@clarkson.edu

INTRODUCTION

Polar stratospheric clouds (PSCs) play a critical role in ozone destruction in the wintertime polar vortex by providing surfaces for chlorine activation and removing nitric acid from the gas phase (Solomon et al. 1986; WMO 1999). PSCs exist in the liquid (supercooled ternary solutions) and solid (ice crystals, nitric acid hydrates) phases. The thermodynamics of PSC particle formation and growth has been studied in laboratory experiments (Hanson and Mauersberger 1988; Carslaw et al. 1994), but accurate atmospheric measurements are still required to verify the applicability of these mechanisms and rates for atmospheric processes. Measurements of particle size, number density, and

composition are critical to better constrain the ozone loss mechanisms. Analysis of in situ particle measurements made using aircraft instruments in general requires the knowledge of the instrument sampling characteristics over the wide range of PSC particle diameters (0.1–20 μm; Dye et al. 1992; Fahey et al. 2001). Measurements during the NASA SAGE-III ozone loss validation experiment (SOLVE) in the 2000 Arctic winter revealed a new large class of HNO_3-containing PSC particles (Fahey et al. 2001; Northway et al. 2002; Brooks et al. 2003). The measurement analysis relied on the knowledge of the particle sampling efficiencies (presented here) for a range of particles for the NOAA NO_y instrument inlet located on the NASA ER-2 high-altitude aircraft.

Particle sampling from aircraft, can either be isokinetic or anisokinetic. The inlet is classified as isokinetic if the sampling velocities match that of the freestream and as anisokinetic if they do not. Isokinetic sampling ensures a particle concentration in the inlet that is generally representative of the concentrations in the freestream. Anisokinetic sampling can enhance or reduce particle concentrations in comparison to the freestream values, depending on whether the sample air velocity in the inlet is less or more than the aircraft speed, respectively. Anisokinetic sampling is sometimes used to extend the range of measurements when the ambient aerosol concentrations are too low or too high for direct measurements. The concentration enhancement or reduction in an anisokinetic inlet is, however, particle size–dependent and must be determined to enable accurate analysis of atmospheric measurements.

This study assesses the sampling characteristics of the inlets of the NOAA NO_y instrument based upon computational fluid dynamic (CFD) flow simulations. This instrument measures reactive nitrogen (NO_y) in the sample flow. For stratospheric measurements, NO_y is the sum of NO, NO_2, HNO_3, $ClONO_2$, $2x(N_2O_5)$, and HO_2NO_2. During the SOLVE campaign, concentrations of NO, NO_2, N_2O_5, and HO_2NO_2 were very low, and hence NO_y measurements are representative of the concentrations of HNO_3 and $ClONO_2$ in the sampled air.

The design and application of the instrument and inlet have been described previously and the instrument has been used in several field campaigns (Fahey et al. 1989; Kelly et al. 1989; Gao et al. 1997; Del Negro et al. 1997). During the SOLVE 2000 campaign (Newman et al. 2002) NO_y was measured using four inlets with different particle sampling characteristics (Fahey et al. 2001; Northway et al. 2002). The NO_y inlet housing (Figure 1) is suspended approximately 50 cm (centerline) below the equipment bay, forward of the wings in the ER-2 fuselage. The housing shape is a double ellipse of revolution approximately, 76 cm long and resembles an American football (referred as *the football* hereafter; Northway et al. 2002). There are four forward-facing inlets projecting out of the football surface, (1) an on-axis front inlet and (2) three off-axis rear inlets. The latter group (referred to as *rear inlet*), which extend left, right, and downwards with respect to the direction of motion, provide equivalent gas and particle sampling. The flow and particle behavior around the football determine the sampling characteristics of the front and rear inlets. The front inlet projects 1.9 cm from the football surface and samples particles of all sizes. The rear inlet has the same dimensions as that of the front inlet and is located 69 cm downstream of the front inlet and extends ~1.7 cm from the surface. The football acts a particle separator by inertially removing large particles from the air sampled by the rear inlet. To estimate the sampling characteristics of the two inlets, the flow field and the resultant particle trajectories around the football were calculated in this study.

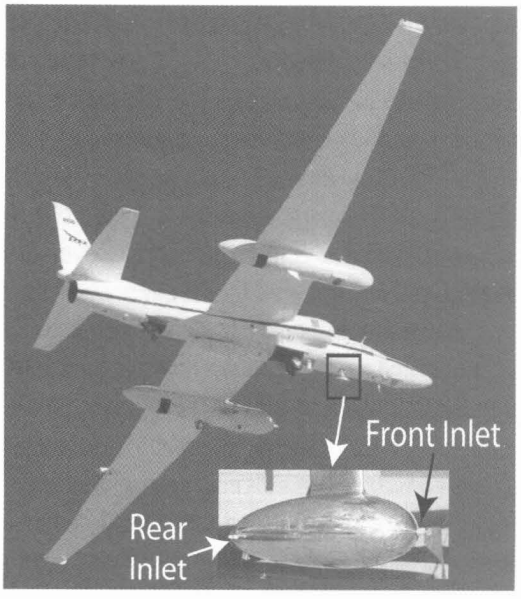

Figure 1. The NO_y instrument on the ER-2 aircraft and the position of the front and rear inlets on the instrument.

Flow around the football is similar, in principle, to flow around an aircraft fuselage. Particle trajectories in the flow around the aircraft have been studied theoretically and experimentally (King 1984a, b; Geller et al. 1993). Kelly et al. (1989) and Fahey et al. (1989) used the theoretical work of King et al. (1984a) to estimate the cut size of the rear inlet as 5.0 μm for spherical ice particles (1 g cm^{-3}). That analysis was, however, based on potential flow calculation and did not consider either the compressibility effects on the flow or the noncontinuum effects on particle drag that are encountered while sampling from the ER-2 aircraft in the stratosphere. The front inlet was used for the first time during SOLVE 2000 for particulate NO_y measurements (Fahey et al. 2001; Northway et al. 2002), and its particle-sampling characteristics have not been simulated prior to this work. The presence of the football blunt body behind the front inlet alters its sampling characteristics, making it different from that of a cylindrical pipe probe sampling anisokinetically from freestream (Rader and Marple 1988). Accurate estimation of particulate contribution to the NO_y signal of the two inlets requires the knowledge of the inlet sampling characteristics, i.e., particle cut-size and size-dependent enhancement factors.

MODELING

We used the CFD program FLUENT (FLUENT Inc., NH, USA) to model flow around the football and calculate particle

trajectories sampled by the inlets. FLUENT uses a finite-volume formulation (Patankar 1980) to solve the mass, momentum, and energy conservation equations and has been used earlier in similar flow conditions (Adamopoulos and Petropakis 1999; Yilmaz and Cliffe 2000; Dhaniyala et al. 2003). Because the NO_y instrument is flown on a high-speed aircraft (ER-2, speed ~0.7 Mach), the air has to be treated as compressible. The Reynolds number based on the flight velocity and the length scale of the football is high, so a turbulent boundary layer will develop. Turbulent transport is modeled using the single-equation Spalart-Allmaras model (Spalart and Allmaras 1992). The modeled turbulence affects the effective viscosity near the football surface and thus the flow field and particle trajectories near the rear inlet. The football is nominally directed to be aligned to the local flow field. This, in conjunction with the axial symmetry of the external surface of the football surface is used to reduce the model domain to two dimensions.

The flow around the football is largely unaffected by the aircraft because the football is located outside the aircraft boundary layer. The aircraft is, therefore, not considered in the flow simulations. A large computational domain is chosen to enable an appropriate choice of ambient pressure, temperature, and freestream velocity as far-field boundary conditions. A higher resolution griding is used in regions where the velocity gradients are large, such as close to the football surface and near the inlet locations. The front inlet is represented explicitly in the computational model. Simulating the flow field with the off-axis rear inlet, however, requires a three-dimensional domain because the surface is no longer axially symmetric. Significant computational effort will, however, be required for such calculations and is not attempted here. Instead, a two-step approach is used (described later in the Results section) to obtain accurate rear inlet sampling characteristics with two-dimensional simulations.

The 0.4 cm inner diameter NO_y inlets sample at a constant mass flowrate of 1 slpm. The resulting pressure-dependent mean flow velocity in the inlet is about 14 m s^{-1} at 50 hPa and 200 K. This differs from the sampling velocity values used in Fahey et al. (1989), where the velocities in the inlet were obtained assuming static (freestream) pressure rather than a calculated pressure in the inlet. In this work, the mass flow in the inlet is constrained by setting appropriate pressure outlet boundary condition at a notional inlet exhaust. The slower flow in the inlet compared to the freestream velocity (~200 m s^{-1}) results in the anisokinetic sampling of ambient particles. Particles of smaller diameters (<0.1 μm) are sampled along with the airmass, but large particles (>1 μm) are inertially brought into the inlet from outside the sampled airmass.

To test particle trajectory calculations, we have simulated the anisokinetic sampling characteristics of a thin-wall cylindrical pipe. Particle enhancement factors (EF) for a thin-wall pipe have been shown empirically to follow the relationship (Belyaev and Levin 1974)

$$EF_v = 1 + \left(\frac{U_0}{U} - 1\right)\left(1 - \frac{1}{(1 + B\,\mathrm{Stk})}\right), \qquad [1]$$

where U_0 is the freestream or aircraft velocity, U the inlet flow velocity, and the function B was obtained empirically as

$$B = 2 + 0.617\frac{U}{U_0}, \qquad [2]$$

and Stk, the Stokes parameter, is

$$\mathrm{Stk} = \frac{\rho_p D_p^2 C_c U_0}{18\,\mu d}, \qquad [3]$$

where ρ_p is the particle density, D_p is the particle diameter, C_c is the Cunningham slip correction factor, μ is the dynamic viscosity of air, and d is the inlet diameter.

The above equation for particle enhancement (EF_v) represents the increase in the volumetric particle number concentration (number of particles per cm^3) in the inlet compared to that in the freestream. The particle enhancements can also be represented on a mass basis (mass of aerosol per mg of air) by accounting for the increase in gas density in the inlet compared to the ambient. The particle enhancement on a mass basis (EF_m) is related to the particle number concentration enhancement (EF_v) as

$$EF_m = EF_v\frac{\rho_\infty}{\rho}, \qquad [4]$$

where ρ_∞ is the gas density in the freestream and ρ is the gas density in the inlet corresponding to the inlet pressure. EF_m must be used to account properly for enhancements in NO_y mixing ratios when sampling PSC particles (Northway et al. 2002). If number densities of sampled particles are being measured, EF_v is used as the enhancement factor with appropriate modifications for pressure changes between the inlet opening and the sampling point downstream. We note in passing that EF_v, calculated using Equation (1) with an inlet pressure equal to the freestream pressure, is equivalent to EF_m. EF_m was calculated in this way in the Fahey et al. (1989) analysis of aerosol enhancement for the football inlets.

The presence of particles is not considered in the CFD flow simulations. This approach is valid because particle sizes of interest (0.1–20 μm) are small compared to inlet dimensions. Also, the number concentrations (<100 cm^{-3}) are too small to influence flow characteristics. Particles are seeded well upstream of the inlet, where flow is unaffected by the presence of the football. To seed uniform upstream particle concentration, particles are injected into several small intervals spaced uniformly in the radial direction. The areas enclosed by these intervals increase with their increasing radial distance from the

Table 1
Modeling parameters for simulations with thin-wall pipe and football NO_y inlets

Flow				Particles	
Pressure (hPa)	Freestream velocity m s^{-1}	Inlet velocity m s^{-1}	Temperature (K)	Diameter (μm)	Density (gm cm^{-3})
50	200	14	200	0.1–100	1.62
70	200	10	200	0.1–100	1.62
90	200	7.8	200	0.1–100	1.62
100	200	7	200	0.1–100	1.62

axis. Thus, to obtain uniform upstream particle concentration, the particle numbers in the intervals are scaled corresponding to their areas.

The particle positions along the flow are tracked by solving for the Stokes drag assuming spherical shaped particles. Because the football is usually used for measurements in the stratosphere (pressure ~50–100 hPa), noncontinuum effects are important in calculating particle trajectories and are accounted for here by considering local pressures. The enhancement factors (EF_v and EF_m) for the front and rear inlets are obtained as a ratio of the particle concentration in the inlets to that in the freestream. Brownian diffusion of the particles can be neglected in the simulations because the Peclet numbers for even smallest particle sizes considered (0.1 μm) are very large (~10^7).

RESULTS

The initial flow and particle simulations were performed for a thin-wall pipe sampling from freestream for conditions similar to that encountered by the football (as listed in Table 1). The pipe dimensions are chosen to be the same as those of the NO_y inlets (ID 0.4 cm). The particle density is chosen to be that of nitric acid trihydrate (NAT; 1.62 g cm^{-3}). The gas pathlines and particle trajectories (diameter 1 μm) obtained for simulations of anisokinetic sampling by a thin-wall pipe are shown in Figure 2 for an ambient pressure of 50 hPa. The limiting pathlines and particle trajectories, representing the boundaries of the sampled airmass and sampled particles, respectively, are highlighted in the figure. The cross section of the limiting particle trajectories is larger than that of the limiting pathlines, resulting in the enhancement of these particles in the inlet. Particle number concentration in the inlet is obtained by calculating the number of particles trapped in the inlet for unit volume of air sampled. The enhancement factors obtained from the simulations largely match empirical values (Equation (1)) for particle sizes larger than 10 μm (enhancements are ~U_0/U) and for the smallest particle sizes (enhancements ~1; Figure 3). A small discrepancy is observed between the empirical values and simulation results for particle sizes between 0.1 and 0.5 μm. This is possibly due to several reasons, including the following:

- The test conditions of freestream-to-sampling velocity are 14.2 (50 hPa) and 20 (100 hPa), both higher than the validity range of the empirical equation (ratio of 6 or lower).
- The empirical curves were obtained from experimental measurements made under continuum conditions, and for the smallest particles the effect of gas slip can emphasize inertia and result in deviations from the empirically predicted values.

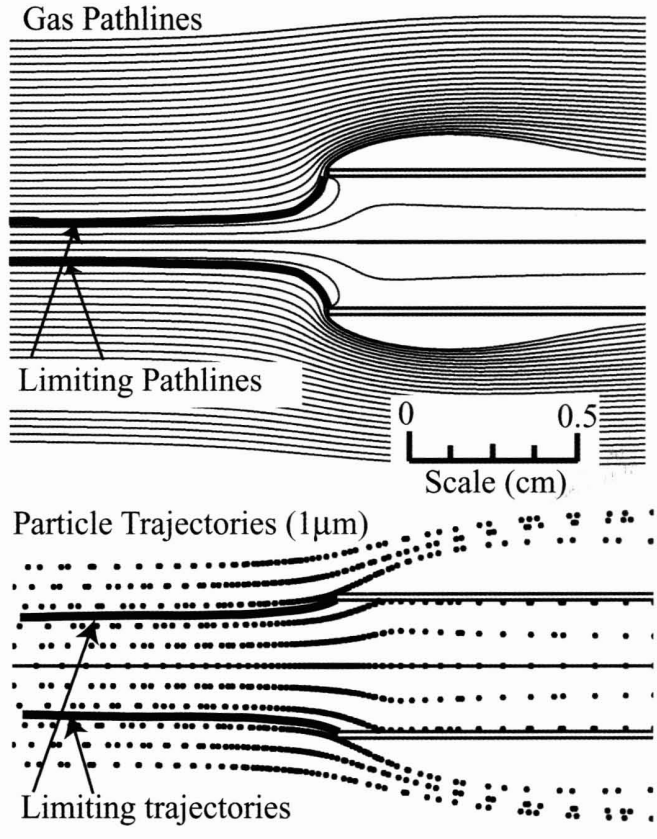

Figure 2. Gas pathlines and particle trajectories near the pipe inlet for freestream conditions of Temperature = 200 K, Pressure = 50 hPa, and Velocity = 200 m s^{-1}, and an inlet sample flow of 1 slpm. The limiting pathlines and particle trajectories (1 μm) are highlighted, illustrating particle concentration enhancement due to anisokinetic sampling.

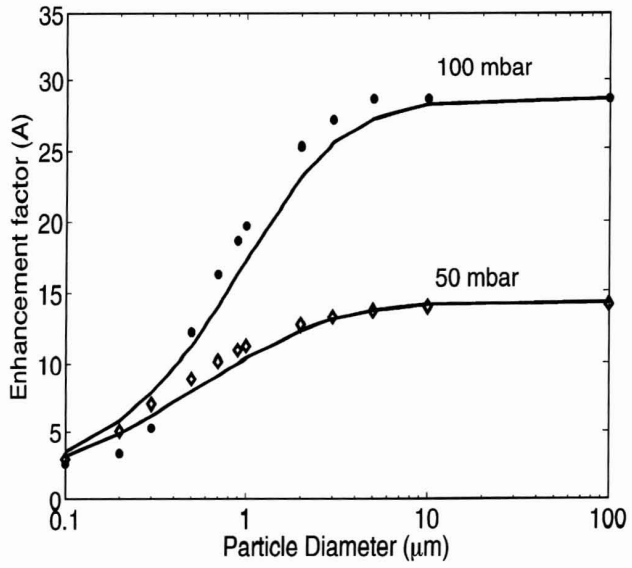

Figure 3. Empirical correlations (lines) and numerical predictions (symbols) of particle number enhancement (A) in a thin-walled pipe in freestream. Freestream conditions: Pressure = 50, 100 hPa, Temperature = 200 K, Velocity = 200 m s^{-1}, and an inlet sample flow of 1 slpm. Note that to calculate particle mass enhancement per unit mass of sampled air, the gas density increase in the inlet must be considered (Equation (4)).

- The effect of gas slip to emphasize particle inertia also explains the increased sampling of smaller particles at 50 hPa in comparison to that at 100 hPa.

Simulations of flow around the football reveals the expected pressure increase near the front inlet due to flow stagnation (Figure 4). Corresponding to the increasing pressure as the flow approaches the inlet, the temperatures increase due to ram heating and warm to the stagnation temperature in the inlet (Figure 5). The high-pressure region alters the streamlines further upstream of the football front inlet than for a thin-wall pipe. Thus, particle trajectories in the vicinity of the front inlet and inlet sampling characteristics also differ from that of the thin-wall pipe.

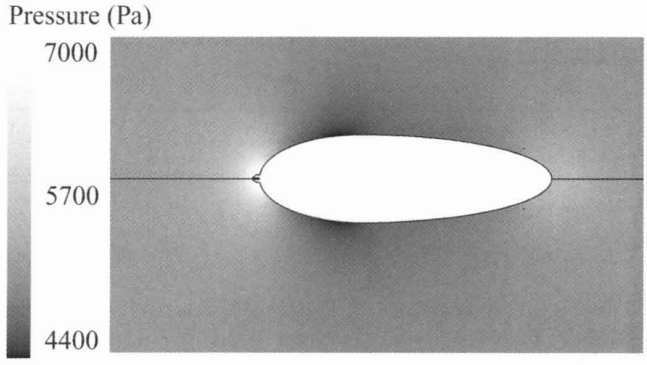

Figure 4. Static pressures in the vicinity of the football. Freestream conditions: Temperature = 200 K, Pressure = 50 hPa, and Velocity = 200 m s^{-1}.

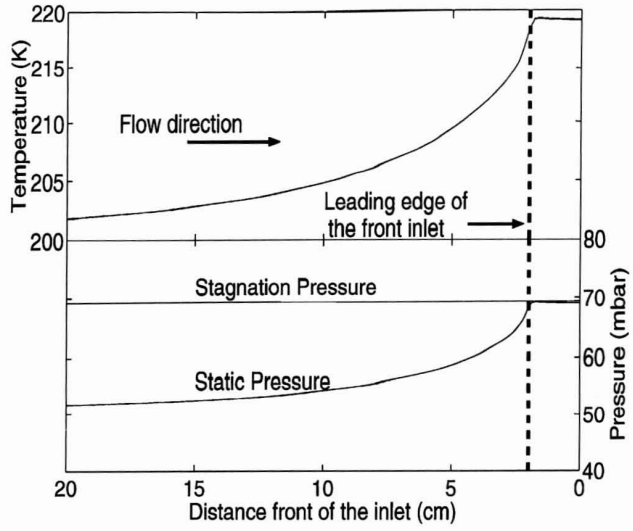

Figure 5. Pressure and temperature variation for flow along the axis approaching the football front inlet. Freestream conditions: Temperature = 200 K, Pressure = 50 hPa, Velocity = 200 m s^{-1}, and an inlet sample flow of 1 slpm.

The front inlet sampling characteristics can be obtained from the calculated two-dimensional flow field around the football using the same approach as that described for the thin-wall pipe. For the rear inlet, however, its off-axis location complicates enhancement factor calculations due to the influence of the three-dimensional flow field on the sampled particle trajectories. However, rear inlet sampling characteristics can be accurately obtained without resorting to the computationally intensive three-dimensional simulations, using a two-step approach. In the first step, the effect of the football on the particle concentration at the rear inlet location is calculated (referred to as the rear-inlet-location enhancement factors). In the second step, the enhancements of the rear inlet in freestream without the football is calculated (referred to as the rear-inlet-shape enhancement factors).

The rear-inlet-location enhancement factors are obtained from two-dimensional simulations of flow around the football surface without the presence of the rear inlet. For these calculations, a porous element of the same diameter as the inlet ID is placed at the rear inlet location. The pressure drop across this element is set to zero to ensure that it does not influence the flow, while a particle trap boundary condition is used for enhancement factor calculations. The rear-inlet-location enhancements are then calculated by seeding uniform particle concentrations upstream of the football and calculating particle concentrations at the porous element.

In the second step, rear-inlet-shape enhancement factors are obtained from two-dimensional flow simulations around the rear inlet in freestream (Figure 6). The simulations are performed considering the freestream conditions consistent with the football simulations at different pressure conditions (Table 1). Due to the finite wall thickness of the rear inlet, its sampling characteristics will differ from those of the thin-wall pipe. The rear-inlet-location and rear-inlet-shape enhancement factors are convolved

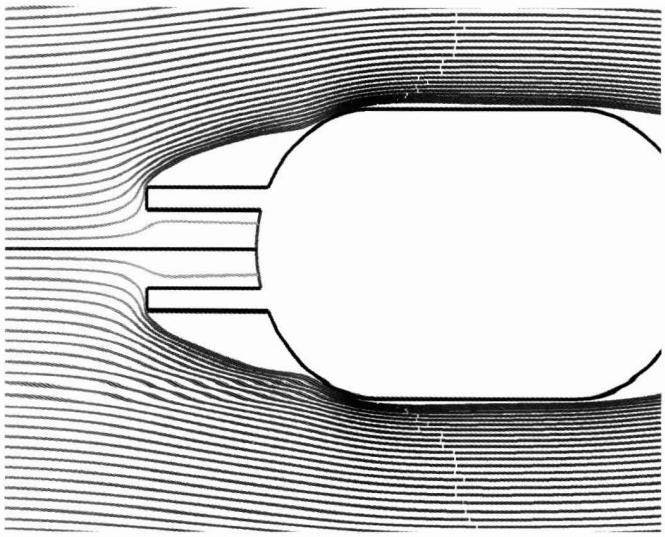

Figure 6. The gas pathlines around the rear inlet sampling in freestream conditions of Temperature = 200 K, Pressure = 50 hPa, Velocity = 200 m s^{-1}, and an inlet sample flowrate of 1 slpm.

to obtain the net enhancement values for the rear inlet as a function of particle size.

The trajectories around the football and in the vicinity of the front and the rear inlet locations are shown for 0.1 and 2.0 μm diameter particles in Figures 7 and 8, respectively. The small particles (e.g., 0.1 μm) largely follow the flow streamlines because they have low inertia and hence their number concentrations are not greatly enhanced in the front inlet. The 2 μm diameter particles have larger inertia (compared to 0.1 μm particles), resulting in their increased sampling in the front inlet. As the flow goes

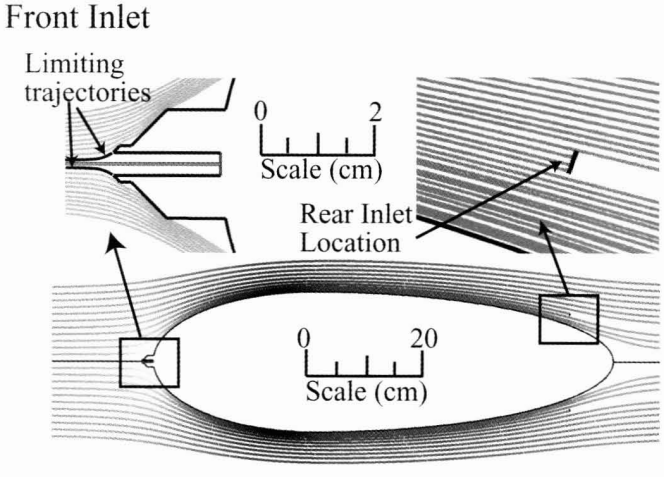

Figure 7. (a) Trajectories of 0.1 μm diameter particles around the football colored by flow velocity. (b) Trajectories in the vicinity of the front inlet with the limiting trajectory highlighted. (c) At the back-inlet location, particle concentrations are similar to the input conditions well upstream of the football. The freestream conditions for these simulations were: Temperature = 200 K, Pressure = 50 hPa, Velocity = 200 m s^{-1}, and an inlet sample flow of 1 slpm.

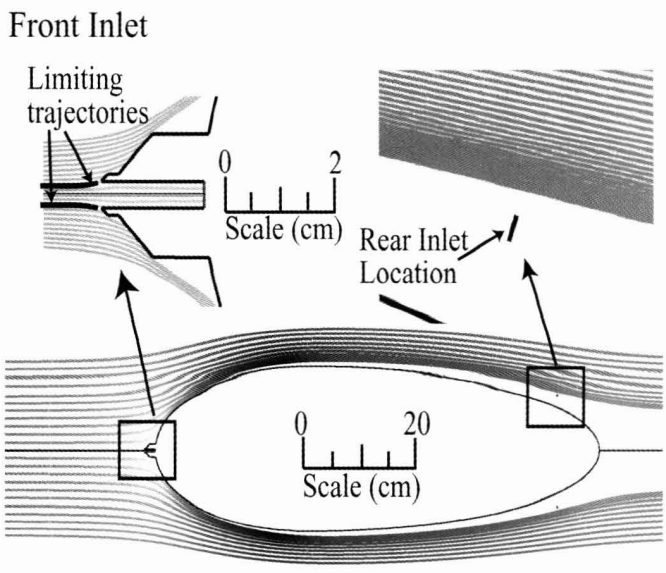

Figure 8. (a) Trajectories of 2.0 μm diameter particles around the football colored by flow velocity. (b) The limiting trajectories of the particles sampled by the front inlet are highlighted, indicating higher sampled numbers than for 0.1 μm particles. (c) Due to the significant inertia of the 2.0 μm particles, they do not follow the narrowing of the football shape and are thus not sampled at the rear-inlet location. The freestream conditions for these simulations were Temperature = 200 K, Pressure = 50 hPa, Velocity = 200 m s^{-1}, and an inlet sample flow of 1 slpm.

past the front inlet, particles with low inertia (Stokes number < ~0.5) largely follow the flow towards the rear inlet location. For large particles (>~2.0 μm diameter), due to their significant inertia the particles just outside the front-inlet limiting trajectories impact on the football surface, and those that go past the football front surface, are unable to follow the narrowing of the football shape. As a result, these particles are not sampled at the rear inlet. Particles in the intermediate size range (~ 0.9–2 μm) are inertially concentrated as they pass around the football and are thus sampled more efficiently at the rear inlet. These rear-inlet-location enhancements are plotted in Figure 9. Similar observations of particle enhancement around blunt bodies have been made from studies of flow around aircrafts (King 1984a; Geller et al. 1993).

The rear-inlet-shape enhancement factors obtained from simulations of rear inlet in freestream are also shown in Figure 9 for different freestream pressure conditions. The finite wall thickness is seen to lower the enhancements over the entire size range of interest at the back inlet. The net rear inlet enhancement factor is obtained by convolving the rear-inlet-shape and rear-inlet-location enhancement factors.

The net volumetric enhancement factors for the front and rear inlets are shown as function of particle size in Figure 10. In Fahey et al. (1989), the rear inlet particle cutoff size was predicted to be ~5 μm (for ice particles of density 1 gm cm^{-3} at 100 hPa). However, this study shows that particles larger than 2 μm (~2.5 μm at 100 hPa for particle density of 1 g cm^{-3})

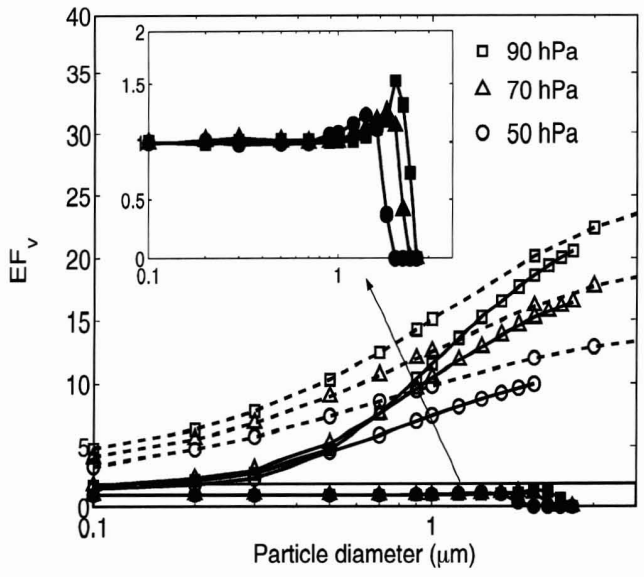

Figure 9. The calculated rear-inlet-shape and rear-inlet-location enhancement factors (EF_v) are plotted as a function of particle size for a range of static pressures. The calculated rear-inlet-shape enhancement factors (solid lines with open symbols) are seen to be lower than the empirically predicted values (Equation (1); dashed lines in this figure). The rear-inlet-location enhancement factors (inset plot) indicate that concentrations of a narrow range of particles are enhanced at the rear inlet. The two rear-inlet enhancement factors are convolved to obtain the net enhancement factor.

are not sampled by the rear inlet. The earlier calculations, based on the work of King (1984a), did not consider the effects of compressibility on the flow field or the inertial enhancement of particle concentrations due to flow around the football. In addition, the Knudsen numbers (Kn) suggest that the flow around the particles is in the slip flow regime ($Kn > \sim 10^{-3}$), but these non-continuum effects were not accounted for in the particle drag calculations. The gas slip on the particle surface lowers drag, resulting in enhanced inertial separation of particles. At higher ambient pressures, the slip effect on particle drag is reduced, and the particle cut-size is shifted towards larger sizes. The front inlet enhancement factors deviate from the empirical prediction for sizes below 10 μm. The presence of the blunt body results in lower particle enhancements, compared to empirical predictions for a pipe in freestream. Also, the finite dimensions of rear inlet affects its sampling characteristics and was not considered before.

The differences between the enhancement results presented here (Figures 10 and 11) and those presented in Figure 2 in Northway et al. (2002) are due to the differences in the calculations of the back inlet enhancements. In Northway et al. (2002), the rear-inlet wall thickness was not considered, and the rear-inlet-shape enhancement factors were assumed to be the same as that of a thin-wall pipe in freestream.

PARTICLE THERMODYNAMICS MODELING

Experimental verification of model results are difficult due to the high-speed, compressible flow conditions and the problems of seeding particles in such flows. Some predictions of this study, however, can be tested using data obtained from the SOLVE campaign. The flow simulations predict that for ambient particle sizes between 0.5 and ~1 μm, enhancement factors are greater for the rear inlet than for the front inlet. This prediction is important for understanding the limitation of data analysis using the difference of front- and rear-inlet measurements as representative of aerosol-phase NO_y. Testing this prediction with SOLVE data requires instances where a significant population of PSC particles are in the size range of 0.5 to 1 μm

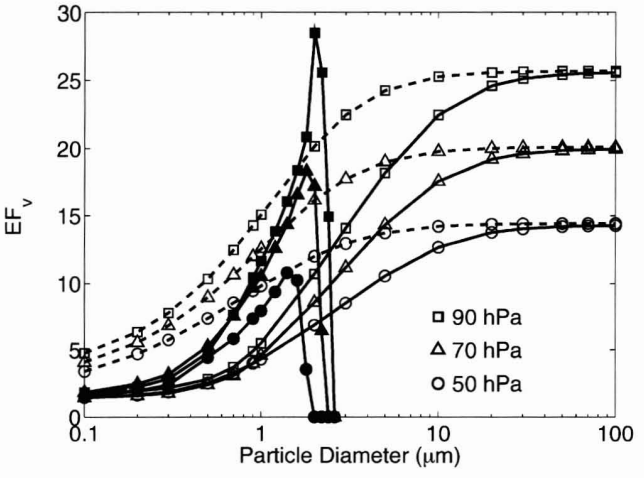

Figure 10. Calculated volumetric particle enhancements (EF_v) for the rear (solid lines with solid symbols) and front (solid lines with open symbols) inlets for varying ambient pressures compared with the corresponding empirical enhancement values for a pipe (dashed lines).

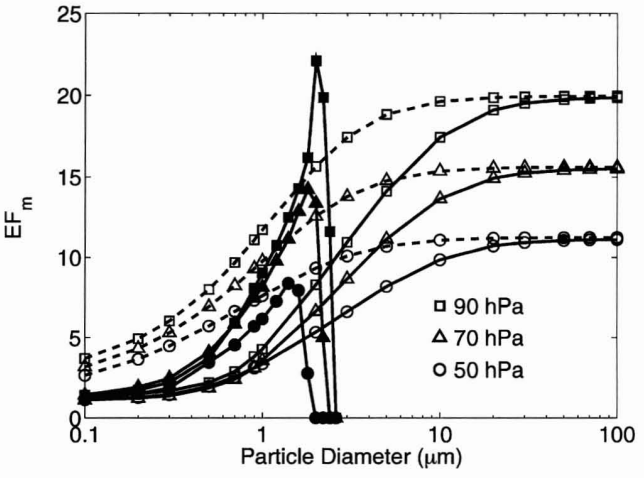

Figure 11. Calculated mass particle enhancements (EF_m) for the rear (solid lines with solid symbols) and front (solid lines with open symbols) inlets for varying ambient pressures. The empirical enhancement values for a pipe are shown for comparison (dashed lines).

diameter with few or no particles larger than 2 μm. PSCs exist in both liquid and solid phases (Toon et al. 2000). The liquid droplets, called *super-cooled ternary solutions* (STS), typically have a mean size around 0.2 μm at warm temperatures (Del Negro et al. 1997) and grow with the uptake of nitric acid and water as temperatures cool to below 193 K (at 50 hPa; Carslaw et al. 1994). The solid-phase PSCs are typically nitric acid hydrates (NAHs). NAHs have lower HNO_3 vapor pressures and, hence, are likely to grow faster than super-cooled ternary solutions (STS) under typical polar stratospheric conditions and usually have diameters greater than 1 μm. The conditions for testing modeling results require that the only particles present are the STS, growth-limited NAHs, or both.

The cold polar stratospheric conditions during the first ER-2 SOLVE deployment (January and early February 2000) resulted in a significant large-diameter (>2 μm) particle population with an assumed composition of NAT (Fahey et al. 2001; Northway et al. 2002; Mckinney et al. 2004), rendering this particle data set inappropriate to test the current modeling predictions. During the second deployment in February and March, the polar vortex conditions were such that large NAT particles were less abundant and temperatures along the ER-2 flight track were often higher (>195 K), resulting in low particulate NO_y mass. Appropriate conditions for the analysis of the NO_y inlet performance existed on February 26 when ambient temperatures were cold (<193 K), and yet very few large particles (diameter >2 μm) were present. The cold temperatures suggest that a significant fraction of STS particles would have grown to the size range of interest (0.5–1.0 μm), while the absence of large particles suggests that NAHs were not present. Therefore, particle thermodynamic modeling considering only STS compositions will provide a good estimate of the sampled particle size distribution.

In our thermodynamic modeling, the background sulfate particles are assumed to have a lognormal size distribution with mean size, standard deviation, and total number obtained from the observations of NMASS and FCAS for February 26 (mean size = 0.08 μm, σ_g = 1.8, number concentration = 10 cm^{-3}; consistent with Drdla et al. 2002). The evolution of this background size distribution is modeled by assuming equilibrium growth of STS particles considering the measured ambient conditions (temperature, water vapor, and HNO_3) and the noncontinuum particle growth equations (Pruppacher and Klett 1978; Hinds 2001). Back trajectory calculations reveal that the sampled cold air masses (temperature < 193 K) experienced significant cooling over a 24 h period prior to the sampling time. Over a 6 h period the cooling rate for the air masses was ~4–8 K/day (Figure 12). The time constants for HNO_3 uptake onto STS particles in the diameter range of 0.7–1 μm is ~1–6 h (Meilinger et al. 1995). The fast cooling rates and the slow HNO_3 uptake by particles results in nonequilibrium STS compositions. To account for this, STS compositions are calculated using temperatures that are 1°C higher than the ambient values, consistent with the mean airmass temperatures where particles resided 3–6 hours prior to their sampling.

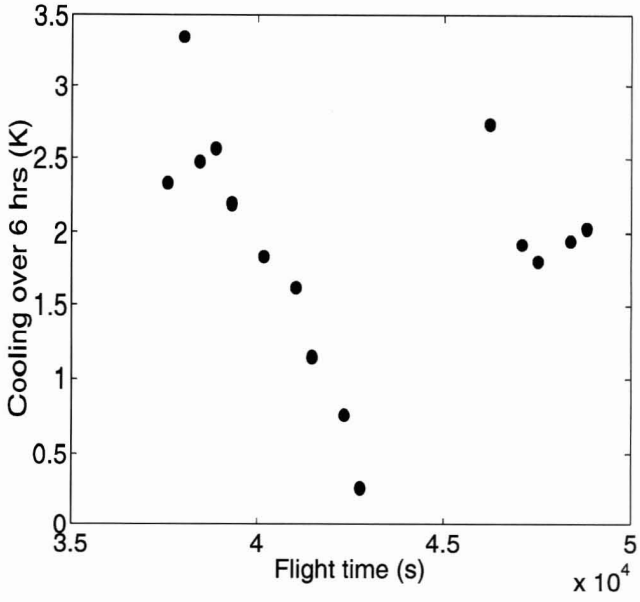

Figure 12. The cooling experienced by the sampled airmass over a 6 h period prior to sampling. Data is shown for flight times where the observed temperatures were <192.5 K.

In our simulations, an initial value of the total HNO_3 concentration is assumed and STS thermodynamics is used to partition the total HNO_3 between the aerosol and gas phase. The aerosol-phase HNO_3 is distributed over the background particles to obtain the STS particle size distributions (similar to the approach of Del Negro et al. 1997). The calculated STS particle size distribution is then used in conjunction with the rear-inlet enhancement factors, gas-phase HNO_3, ambient water partial pressures (from the Harvard Lyman alpha hygrometer instrument), and $ClONO_2$ values (Stimpfle et al. 2004) to calculate the rear inlet NO_y values. The difference between the calculated and measured rear-inlet NO_y is then used to scale the assumed total HNO_3 concentration, and the calculation procedure is repeated with the new total HNO_3 concentration. The model is iterated until convergence of total HNO_3 is obtained. The front inlet NO_y concentration is then calculated considering the particle size distribution, front-inlet enhancements, ambient water partial pressures, and the calculated total and gas-phase ambient HNO_3 concentrations. This procedure is repeated for all measurement data points.

The calculated and measured NO_y values for the two inlet channels of the football instrument are shown in Figure 13. Two particularly interesting time intervals are highlighted (inset figures) where the measured NO_y in the front inlet is less than that in the rear inlet. This increased NO_y sampling at the front inlet is also predicted by our calculations considering STS thermodynamics and the inlet enhancements. The difference between the front- and rear-inlet NO_y measurements is seen to increase as temperatures cool below 193 K (Figure 14). This is due to the increased uptake of HNO_3 and H_2O by STS particles at colder temperatures resulting in their growth to sizes for which the rear-inlet enhancements are larger than that of the front inlet.

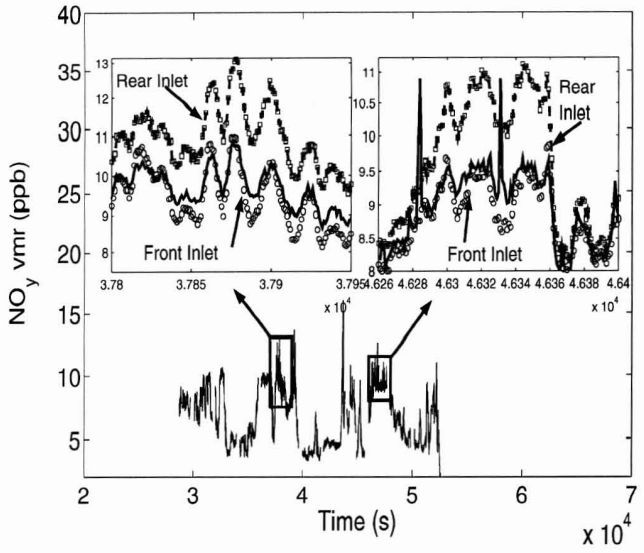

Figure 13. NO_y measurements by the football inlets during the SOLVE mission for the flight on 26 February 2000 reveal instances where the rear inlet oversamples in comparison to the front inlet (inset plots). Simulations of NO_y concentrations in the inlets (symbols) obtained from thermodynamic modeling of STS particle growth in conjunction with the calculated inlet enhancement factors are seen to match observations (lines).

The calculated NO_y differences between the two inlets is seen to largely match observations (Figure 15).

The CFD simulations and thermodynamic modeling results suggest that even a small aerosol mass in the size range of 0.7–2.0 μm can result in significant particulate HNO_3 (and hence NO_y) contribution to the rear-inlet signal. The ambient gas-phase HNO_3 values calculated from thermodynamic modeling can be compared with the HNO_3 values obtained from the rear-inlet NO_y measurements (after accounting for $ClONO_2$ contribution, Figure 16). For warmer temperatures (>~193 K), it is observed that the particulate HNO_3 contribution to the rear-inlet measurements is insignificant. But at colder temperatures, the increased partitioning of HNO_3 into the aerosol phase can result in a significant particulate contribution (up to 4–5 ppb or ~80% of gas-phase concentrations for the analyzed data set) to the rear-inlet measurements. These preliminary calculations suggest that rear-inlet measurements can be

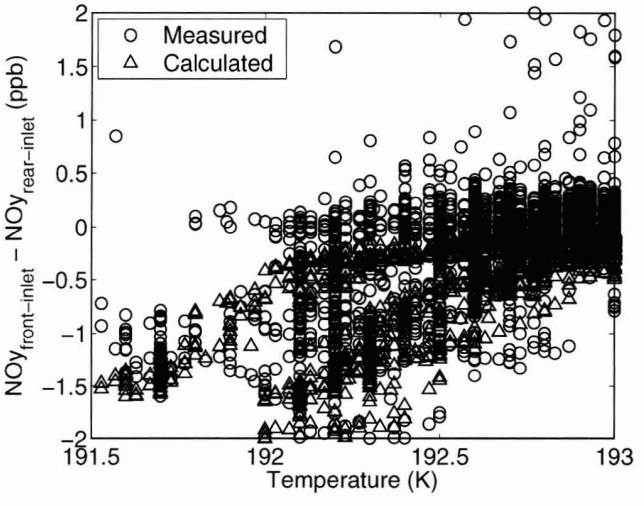

Figure 14. As temperatures cool, the rear inlet is observed to oversample NO_y and the calculated differences of the front- and rear inlet NO_y are seen to largely match the trends of measured values.

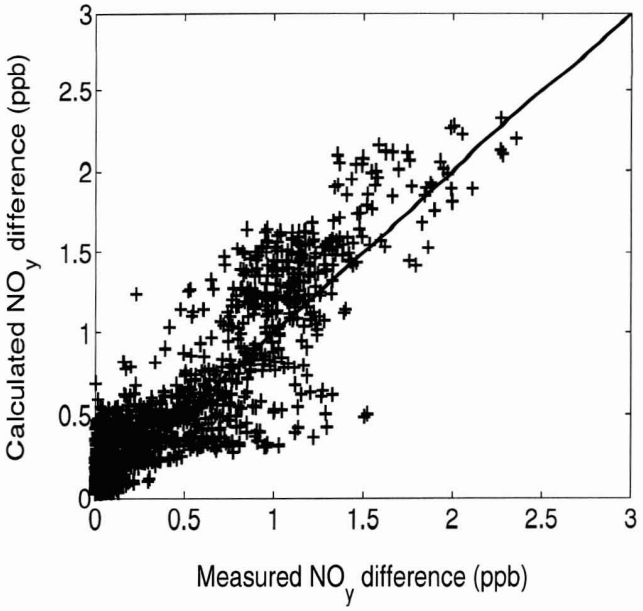

Figure 15. The comparisons of the calculated NO_y differences between the front and the rear inlets match closely with the measured values.

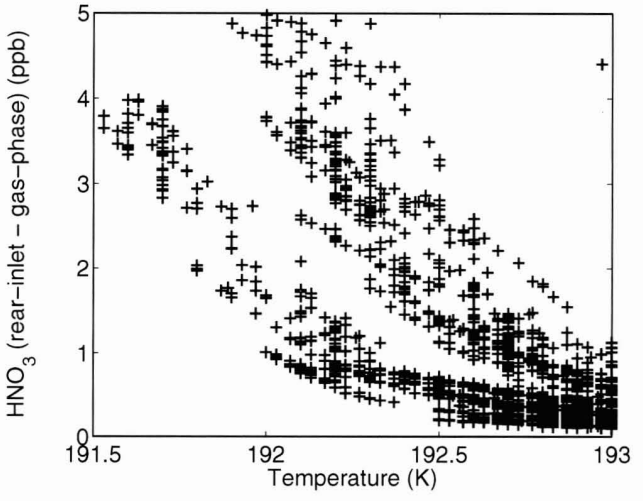

Figure 16. The difference of HNO_3 concentrations calculated from the rear-inlet measurements of NO_y and gas-phase HNO_3 values calculated from the thermodynamic modeling are shown as a function of temperature. The growth of STS particles at colder temperatures and oversampling of particles in the size range of 0.9–2.0 μm results in significant contribution of particulate HNO_3 to the rear-inlet measurements as temperatures cool below 193 K.

assumed to represent gas-phase concentrations only at warm temperatures.

The thermodynamic modeling results provide preliminary validation of the calculated inlet enhancement factors. More detailed modeling considering nonequilibrium growth of NAT and STS particles will enable extracting gas-phase information from the NO_y data for the entire SOLVE campaign. Gas- and aerosol-phase HNO_3 data from the Caltech CIMS instrument for the February 26 flight were not available for comparisons with these results.

CONCLUSIONS

CFD calculations have been used to determine particle sampling characteristics of the two inlets on the NO_y football instrument. The rear inlet is calculated to have a cut size <2 μm. The presence of the football blunt body results in a smaller enhancement of submicron-sized particles in the front inlet than in a pipe sampling from freestream. The blunt body also acts to inertially concentrate particles in a small size range (0.7–1.0 μm under stratospheric sampling conditions), resulting in an oversampling of these particles by the rear-inlet, thus complicating data analysis of the rear-inlet NO_y under certain circumstances.

Preliminary verification of the CFD simulation results was possible using data from the SOLVE 2000 campaign. Measurements of NO_y on 26 February 2000 revealed that majority of the particles sampled on that day were STS. Using a simple STS thermodynamics model in conjunction with the calculated inlet characteristics, the front-inlet NO_y values were calculated and seen to be broadly in agreement with measurements. The predicted oversampling of the 0.5–1.0 μm particles in the rear inlet is observed in the NO_y measurements, and thermodynamic modeling with STS particles provides preliminary validation of the calculated size range over which the rear inlet is likely to oversample. The calculated inlet enhancement factors and thermodynamic modeling results show that an estimation of gas-phase HNO_3 is possible from the two NO_y channels.

REFERENCES

Adamopoulos, K. G., and Petropakis, H. J. (1999). Simulation of Distribution of Discrete Inert Particles in Two Phase Supersonic Mixing, *J. Food Eng.* 42(1):59–66.

Belyaev, S .P., and Levin, L. M. (1974). Techniques for Collection of Representative Aerosol Samples, *Aerosol Sci.* 5:325–338.

Brooks, S. D., Baumgardner, D., Gandrud, B., Dye, J. E., Northway, M. J., Fahey, D. W., Bui, T. P., Toon, O. B., and Tolbert, M. A. (2003). Measurements of Large Stratospheric Particles in the Arctic Polar Vortex, *J. Geophys. Res.* 108(D20): (Art No. 4652).

Carslaw, K. S., Luo, B. P., Clegg, S. L., Peter, T., Brimblecombe, P., and Crutzen, P. J. (1994). Stratospheric Aerosol Growth and HNO_3 Gas Phase Depletion from Coupled HNO_3 and Water Uptake by Liquid Particles, *Geophys. Res. Lett.* 21:2479–2482.

Del Negro, L. A., Fahey, D. W., Donnelly, S. G., Gao, R. S., Keim, E. R., Wamsley, R. C., Woodbridge, E. L., Dye, J. E., Baumgardner, D., Gandrud, B. W., Wilson, J. C., Jonsson, H. H., Loewenstein, M., Podolske, J. R., Webster, C. R., May, R. D., Worsnop, D. R., Tabazadeh, A., Tolbert, M. A., Kelly, K. K., and Chan, K. R. (1997). Evaluating the Role of NAT, NAD, and Liquid $H_2SO_4/H_2O/HNO_3$ Solutions in Antarctic Polar Stratospheric Cloud Aerosol: Observations and Implications, *J. Geophys. Res. Atmosp.* 102(11D):13255–13282.

Dhaniyala, S., Flagan, R. C., McKinney, K. A., and Wennberg, P. O. (2003). Novel Aerosol/Gas Inlet for Aircraft-Based Measurements, *Aerosol Sci. Technol.* 37(10):828–840.

Drdla, K., Gandrud, B. W., Baumgardner, D., Wilson, J. C., Bui, T. P., Hurst, D., Schauffler, S. M., Jost, H., Greenblatt, J. B., and Webster, C. R. (2002). Evidence for the Widespread Presence of Liquid-Phase Particles During the 1999–2000 Arctic Winter, *J. Geophys. Res.* 108(D5):8318.

Dye, J. E., Baumgardner, D., Gandrud, B. W., Kawa, S. R., Kelly, K. K., Loewenstein, M., Ferry, G. V., Chan, K. R., and Gary, B. L. (1992). Particle-Size Distributions in Arctic Polar Stratospheric Clouds, Growth and Freezing of Sulfuric-Acid Droplets, and Implications for Cloud Formation, *J. Geophys. Res.* 97(D8):8015–8034.

Fahey, D. W., Kelly, K. K., Ferry, G. V., Poole, L. R., Wilson, J. C., Murphy, D. M., Loewenstein, M., and Chan, K. R. (1989). In Situ Measurements of Total Reactive Nitrogen, Total Water, and Aerosol in a Polar Stratospheric Cloud in the Antarctic, *J. Geophys. Res.* 94(D9):11299–11315.

Fahey, D. W., Gao, R. S., Carslaw, K. S., Kettleborough, J., Popp, P. J., Northway, M. J., Holecek, J. C., Ciciora, S. C., McLaughlin, R. J., Thompson, T. L., Winkler, R. H., Baumgardner, D. G., Gandrud, B., Wennberg, P. O.,Dhaniyala, S., McKinney, K., Peter, T., Salawitch, R. J., Bui, T. P., Elkins, J. W., Webster, C. R., Atlas, E. L., Jost, H., Wilson, J. C., Herman, R. L.,Kleinbohl, A., and von Konig, M. (2001). The Detection of Large HNO_3-Containing Particles in the Winter Arctic Stratosphere, *Science* 291(5506):1026–1031.

Gao, R. S., Fahey, D. W., Salawitch, R. J., Lloyd, S. A., Anderson, D. E. Demajistre, R., McElroy, C. T., Woodbridge, E. L., Wamsley, R. C., Donnelly, S. G., Del Negro, L. A., Proffitt, M. H., Stimpfle, R. M., Kohn, D. W., Kawa, R., Lait, L. R., Loewenstein, M., Podolske, J. R., Keim, E. R., Dye, J. E., Wilson, J. C., and Chan, K. R. (1997). Partitioning of the Reactive Nitrogen Reservoir in the Lower Stratosphere of the Southern Hemisphere: Observations and Modeling, *J. Geophys. Res. Atmos.* 102(D3):3935–3949.

Geller, A. S., Rader, D. J., and Kempka, S. N. (1993). Calculation of Particle Concentration Around Aircraft-Like Geometries, *J. Aerosol Sci.* 24(6):823–834.

Hanson, D., and Mauersberger, K. (1988). Laboratory Studies of the Nitric Acid Trihydrate: Implications for the South Polar Stratosphere, *Geophys. Res. Lett.* 15(8):855–858.

Hinds, W. C. *Aerosol Technology: Properties, Behavior, and Measurement of Airborne Particles*, (J. Wiley, New York, 2001).

Kelly, K. K., Tuck, A. F., Murphy, D. M., Proffitt, M. H., Fahey, D. W., Jones, R. L., McKenna, D. S., Loewenstein, M., Podolske, J. R., Strahan, S. E., Ferry, G. V., Chan, K. R., Vedder, J. F., Gregory, G. L., Hypes, W. D., McCormick, M. P., Browell, E. V., and Heidt, L. E. (1989). Dehydration in the Lower Antarctic Stratosphere During Late Winter and Early Spring, 1987. *J. Geophys. Res.* 94(D9):11317–11357.

King, W. D. (1984a). Air Flow and Particle Trajectories Around Aircraft Fuselages. I: Theory, *J. Atmos. Oceanic Technol.* 1:5–13.

King, W. D. (1984b). Air Flow and Particle Trajectories Around Aircraft Fuselages. II: Measurements, *J. Atmos. Oceanic Technol.* 1:14–21.

McKinney, K. A., Wennberg, P. O, Dhaniyala, S., Fahey, D. W., Northway, M. J., Kunzi, K. F., von Konig, M., Kullmann, H., Bremer, H., Mahoney, M. J., and Bui, T. P. (2004). Trajectory Studies of Large HNO_3-Containing PSC Particles in the Arctic: Evidence for the Role of NAT, *Geophys. Res. Lett.* 31(Art No. L05110).

Meilinger, S. K., Koop, T., Luo, B. P., Huthwelker, T., Carslaw, K. S., Krieger, U., Crutzen, P. J., and Peter, T. (1995). Size-Dependent Stratospheric Droplet Composition in Lee Wave Temperature-Fluctuations and their Potential Role in PSC Freezing, *Geophys. Res. Lett.* 22(22):3031–3034.

Newman, P. A., Harris, N. R. P., Adriani, A., Amanatidis, G. T., Anderson, J. G., Braathen, G. O., Brune, W. H., Carslaw, K. S., Craig, M. S., DeCola, P. L., Guirlet, M., Hipskind, R. S., Kurylo, M. J., Kullmann, H., Larsen, N., Megie, G. J., Pommereau, J. P., Poole, L. R., Schoeberl, M. R., Stroh, F.,

Toon, O. B., Trepte, C. R., and Van Roozendael, M. (2002). An Overview of the Solve/Theseo 2000 Campaign, *J. Geophys. Res.* 107(D20):8259.

Northway, M. J., Gao, R. S., Popp, P. J., Holecek, J. C., Fahey, D. W., Carslaw, K. S., Tolbert, M. A., Dhaniyala, S., Wennberg, P. O., Lait, L. R., Mahoney, M. J., Herman, R. L., Toon, G. C., and Bui, T. P. (2002). An Analysis of Large HNO_3-Containing Particles Sampled in the Arctic Stratosphere During the Winter of 1999–2000, *J. Geophys. Res.* 107(D20):8298.

Patankar, S. V. (1980). *Numerical Heat Transfer and Fluid Flow*, Taylor and Francis, 1980.

Pruppacher, H. R., and Klett, J. D. 1978. *Microphysics of Clouds and Precipitation*. D. Reidel Pub. Co. Dordrecht, Holland.

Rader D. J., and Marple, V. A. (1988). A Study of the Effects of Anisokinetic Sampling, *Aerosol Sci. Technol.* 8:283–299.

Solomon, S., Garcia, R. R., Rowland, F. S., and Wuebbles, D. J. (1986). On the Depletion of Antarctic Ozone, *Nature* 321(6072):755–758.

Spalart, P., and Allmaras, S. (1992). *A One-Equation Turbulence Model for Aerodynamic Flows*. Technical Report AIAA-92-0439, American Institute of Aeronautics and Astronautics, 1992.

Stimpfle, R. M., Wilmouth, D. M., Salawitch, R. J., and Anderson, J. G. 2004. First Measurements of ClOOCl in the Stratosphere: The Coupling of ClOOCl and ClO in the Arctic Polar Vortex, *J. Geophys. Res.* 109(D3): (Art No. D03301).

Toon, O., Tabazadeh, A., Browell, E., and Jordan, J. (2000). Analysis of Lidar Observations of Arctic Polar Stratospheric Clouds During January 1989, *J. Geophys. Res.* 105:20589–20615.

World Meteorological Organization (WMO). (1999). *Scientific Assessment of Ozone Depletion: 1998 (Rep, 44)*. World Meteorological Organization, Geneva, Switzerland.

Yilmaz S., and Cliffe, K. R. 2000. Particle Deposition Simulation Using the CFD code FLUENT, *J. Inst. Energy* 73(494):65–68.